

# A modeling study of predator–prey interaction propounding honest signals and cues\*

Ahd Mahmoud Al-Salman<sup>1</sup>, Joseph Páez Chávez<sup>2,1</sup>, and Karunia Putra Wijaya<sup>1,\*</sup>

<sup>1</sup>*Mathematical Institute, University of Koblenz, 56070 Koblenz, Germany*

<sup>2</sup>*Center for Applied Dynamical Systems and Computational Methods (CADSCOM), Faculty of Natural Sciences and Mathematics, Escuela Superior Politécnica del Litoral, P.O. Box 09-01-5863, Guayaquil, Ecuador*

\*Corresponding author. Email: [karuniaputra@uni-koblenz.de](mailto:karuniaputra@uni-koblenz.de)

---

Honest signals and cues have been observed as part of interspecific and intraspecific communication among animals. Recent theories suggest that existing signaling systems have evolved through natural selection imposed by predators. Honest signaling in the interspecific communication can provide insight into the evolution of anti-predation techniques. In this work, we introduce a deterministic three-stage, two-species predator–prey model, which modulates the impact of honest signals and cues on the interacting populations. The model is built from a set of first principles originated from signaling and social learning theory in which the response of predators to transmitted honest signals or cues is determined. The predators then use the signals to decide whether to pursue the attack or save their energy for an easier catch. Other members from the prey population that are not familiar with signaling their fitness observe and learn the technique. Our numerical bifurcation analysis indicates that increasing the predator’s search rate and the corresponding assimilation efficiency gives a journey from predator–prey abundance and scarcity, a stable transient cycle between persistence and near-extinction, a homoclinic orbit pointing towards extinction, and ultimately, a quasi-periodic orbit. A similar discovery is met under the increment of the prey’s intrinsic birth rate and carrying capacity. When both parameters are of sufficiently large magnitudes, the separator between honest signal and cue takes the similar journey from a stable equilibrium to a quasi-periodic orbit as it increases. In the context of modeling, we conclude that under prey abundance, transmitting error-free honest signals leads to not only a stable but also more predictable predator–prey dynamics.

**Keywords:** predator–prey interaction, signaling theory, honest signal, cue, social learning, codim–1 bifurcation

---

## 1 Introduction

Biological signal has been one of the fundamental subjects in understanding interactions among animals. Owren *et al.* [1] suggest that a biological signal carries motivational messages, which contain signaler arousal and likely upcoming actions. Smith [2] and Hauser [3] characterize a biological signal as information sharing, which is a way broader than carrying solely emotional-motivational messages. Bugnyar *et al.* [4] give a relying [1] yet less popular definition of a biological signal, that is, *encoded information* about sender’s features and stimuli. Lehmann *et al.* [5] mention that a biological signal represents evolved communication that influences the receiver behavior throughout efficiently altering sender’s information, which in turn affects the cooperative tendencies of the receiver. However, the optimality of signaling for a signaler depends on the receiver’s interpretation, meaning that responses count on the signal [6]. The continuing evolution of biological signals forces signalers and receivers to be engaged in a battle of extracting correct interpretation of the signals. It is not immediately apparent whether or not signals are honest or dishonest, making individuals more conspicuous [7].

Zahavi in [8, 9, 10] argues that biological signals are always honest, and they aim to show off the hidden quality of the signaller to the receiver. Dawkins and Krebs [11, 12] oppose Zahavi’s idealism, claiming that organisms bluff and cheat in their signals when communicating with each other. *Zahavi’s*

*handicap hypothesis* [13, 14, 8] is explained particularly for defending honest and costly signals against such counter-arguments. The essence of the hypothesis is that an individual's quality must "honestly" be signaled to others because signaling is costly. However, Számandó and Penn [15] disagree with this hypothesis for several reasons, mainly because there are versions of the handicap hypothesis, but none of which succeeded in providing theoretical proofs. Although a game-theoretic Evolutionarily Stable Strategy (ESS) model [14], which models the handicap principle in sexual selection, can be excepted from that conclusion, other authors [16, 17, 18, 19, 20] did challenge the model. In [21], the authors provided a first experimental conclusion regarding honesty. Their laboratory experiment using blue jays (*Cyanocitta cristata*) showed that signal's cost stabilizes thus encourages honesty, which in return confirms the handicap hypothesis. The model in [22] describes biological signals as mostly honest, at least when there is a large enough variance in individual's quality. In the realm of animal communication, costly signals are entailed with the consistency of the population and increased predation risk [8]. However, for a signal to be an ESS, its costs should decrease the net gain of signaling in order to maintain the signal reliability [23]. Johnstone and Grafen in [24] argue that despite the importance of the handicap principle in biological communication, it comes with an unrealistic assumption that existing supporting models assume error-free biological communications. A general error-prone evolutionarily stable signaling model of the handicap principle is presented by Johnstone and Grafen in [24], that incorporates a perceptual error. A numerical analysis of such perceptual error in the model is presented in [25]. The bottom line is, regardless of whether the signaling systems are error-prone or error-free, they must be honest at equilibrium [24].

**Honest signal.** The study of biological signals reveals information about the signaller and the receiver, where in the context of the current study, prey and predators. In fact, honest signals elevate the ability of prey to escape an attempt of predation [8, 10]. In other words, honest signals are adaptive behavior of prey to help them convey their alertness and relative escape ability from a predator's attack. Predators then decide whether to use the information to attack or not. Predators may as well assess such individual quality, due to which case the honest signaling continues to evolve. An example of honest signal is *stotting* in Thomson's gazelle, which is acted through jumping highly near to a predator instead of running away. This helps signal gazelle's fitness and give a clear message to the predator that "you cannot catch me" [26]. Among biological signals such as acoustic signals, where animals show themselves by loud vocalization, and aposematic signals, when revealing conspicuous colors and even repeated movements, the freedom from error (honesty) is determined by how useful the information is for the sender and the receiver [27]. A fundamental lack of symmetries in signals communication is derived from the different roles and interests of the signaller and receiver, highlighting the importance of explication study on influential signals rather than informative signals [28].

**Cues.** The behavioral change of animals in conveying information about themselves is significant for both the signaler and the receiver. The behavioral change is considered to be positive when the signaler conveys honest information about its fitness, which in turn benefits both the signaler and receiver. In contrast, it is considered to be negative when the information benefits the receiver exclusively. In studies of animal behavior, a fundamental distinction is created between signals. On the one side is honest signal, which is a perceivable entity that has evolved for a specific purpose of conveying information to alter the receiver's behavior, and on the other side is cue, which is unintentional information disclosed by the signaler benefitting the receiver exclusively. An example of a cue is the rustling sound of a mouse that runs through the underbrush. A predator can apparently use this sound as information that may lead it to the mouse's location. However, this information is primarily produced by the mouse rustling activity rather than developed by learning to transmit information.

The primary objective of this study is to model the impact of honest signals and cues on the sustenance of predator-prey interactions. We propose a two-species predator-prey model with the prey population split into individuals who are capable of transmitting honest signals (experienced) and those who are not (inexperienced). At this point, we declare the assumption that all the transmitted signals from experienced prey are honest. However, these signals are *error-prone*, meaning that they are subject to different interpretations from distinct predator individuals. Signal transmitting is

deemed as a behavioral trait that occurs between experienced and inexperienced prey until the latter attain an experience level and emerge into the veteran population. Such process affects the predator, experienced and inexperienced prey population, albeit in different ways. One of the primary concerns of this study is to describe these effects on the population level.

## 2 Mathematical model

Our primary goal in this section is to build a system of differential equations that govern the population dynamics of a predator-prey system in which experienced prey individuals share their skills in transmitting honest signals with inexperienced prey. Experienced prey individuals are knowledgeable and well-informed, comprising those that are capable of transmitting honest signals against attacks. In other words, they can transmit honest signals to a predator to increase their survival chances. On the other hand, inexperienced prey individuals cannot transmit honest signals but discern signals transmitted by the experienced prey and learn how to evolve their escaping techniques. In the system, the prey population that is constrained only by limited environmental resources, is the only source of nourishment for the predator. Throughout this work, we denote by  $x$ ,  $y$  and  $z$  the density of inexperienced prey, experienced prey and predator individuals, respectively.

### 2.1 Prey population growth in the absence of predators

In realistic ecosystems, the population growth rate cannot be represented without environmental constraints. It may grow exponentially for some time, but they will ultimately curtail owing to ceilings determined by limited resources availability. Since every newborn prey is inexperienced, the exponential growth can be modeled by  $r(x + y)$ , where  $r$  denotes the intrinsic growth rate. The growth term  $r(x + y)$  assumes that both inexperienced and experienced prey are able to reproduce. The competition for logistics can usually be modeled by  $(r/C)x(x + y)$ , where  $C$  denotes the carrying capacity, i.e., the maximal prey density the environment can support. The term  $x(x + y)$  represents the mass-action law accounting for competition or interaction for seizing logistics among  $x$ -individuals and between  $x$ - and  $y$ -individuals. Consequently, the logistic growth model of the prey population in the absence of predator is represented by the following equations

$$\begin{aligned} x' &= r(x + y) - \frac{r}{C}x(x + y), \\ y' &= -\frac{r}{C}y(x + y). \end{aligned} \tag{1}$$

Observe that the entire prey population density  $x + y$  satisfies the standard logistic equation.

### 2.2 Predation effect on the prey population

One of the most important components to interpret a mathematical model of the predator-prey system is functional response. In this study, a predator-dependent functional response is considered where prey abundance changes because of predators' interference. Let  $\beta$  denote the predator's search rate (sometimes referred to as *scanning speed*), determining how much area is covered by one predator per unit time. During a predetermined search time  $T_s$ , the predator is able to cover the area  $\beta T_s$ . Following Holling's work [29], we impose an assumption that on every event of meeting, a prey individual can always be captured by the predator. Thus, the total prey individuals of  $X_c := \beta T_s x$  are successfully captured by one average predator during  $T_s$ . When the aforementioned assumption is dropped, Holling uses an inhibition factor  $k$  such that  $X_c := \beta T_s x^k$  instead, which later sets his functional response of type III. Let  $\tau$  denote the time an average predator needs to "handle" one prey individual (handling time). It is worth mentioning that  $\tau$  also includes the satiation time, food-sharing time, and time of not motivated to hunt (cf. [30]). Then,  $T_h := \tau X_c$  represents the total time needed by one predator to handle the entire captured prey individuals. When  $T := T_s + T_h$  denotes the total time for a predator to search and handle the entire captured prey individuals, we get Holling's type II functional response  $X_c = \beta T x / (1 + \beta \tau x)$ , which measures the total number of captured prey individuals by one

predator during  $T$ . We note that in general,  $\tau \ll T$ . As no conflict among predators during hunting is assumed, the total of  $[\beta T x / (1 + \beta \tau x)] \cdot z$  prey individuals per unit area can successfully be captured by  $z$  predators during the entire time  $T$ , or  $[\beta x / (1 + \beta \tau x)] \cdot z$  individuals per unit area and unit time. Including predation, the  $x$ -dynamics in (1) is corrected as

$$x' = r(x + y) - \frac{r}{C}x(x + y) - \frac{\beta x}{1 + \beta \tau x} \cdot z. \quad (2)$$

At this point, the prey dynamics can be set down by combining the logistic growth with the functional response. The latter is proportional to the prey density but saturates to a certain maximum due to an intrinsic capacity of the predators.

### 2.3 Cue for risk assessment by experienced prey

Similarly as for the inexperienced prey, predation leads to decrease in the experienced prey population, notwithstanding the fact that the functional responses cannot be exactly the same. Although the experienced prey can actively convey information and influence the behaviour of the predator through transmitting honest signals, these signals can still be subject to flaws such as leaving different interpretations from some predator individuals at different ranges. A possibility that an error-prone honest signal may turn into a cue is thus envisaged. Rather than using an inhibition factor like in Holling's type III functional response, this study engineers the parameter  $\rho \in [0, 1]$  indicating the presence of error-prone honest signals:

$$y' = -\frac{r}{C}y(x + y) - \rho \cdot \frac{\beta y}{1 + \beta \tau y} \cdot z. \quad (3)$$

Actual cues are passive, as they unintentionally provide the receiver with information that might be correlated with a high chance of attacking [5]. Many studies in the literature refer cues to as non-evolving biological traits because of their impact on the species [31]. Honest signals are also subject to turning into cues as they highly count on receiver's interpretation [6]. In Thomson's gazelles, for example, actual cues attract predators to come and any honest signal (stotting) performed in less than 40 meters away from predators becomes meaningless [32]. This happens as if the prey individual continuously produces cues. When  $\rho$  is small, an average honest signal contains enough information for the predator to rely on such that the catch is undone [27]. This is when the signal is entirely *error-free*. However, in a blunder or conflicting interest, the maintenance of reliable signals is up to the evolutionary interest of the predator, and therefore, signals become uninformative and turn into cues. That is when the signals contain error and  $\rho$  is close to 1.

### 2.4 Learning boosting the cast for experienced prey

Many studies found that animals can recognize their predators without prior experience. It means that predator recognition is a strong genetic component [33]. Nevertheless, genetically functioned defense patterns could be modified by learning [33]. This response modification that is relative to the experienced prey can be seen as an adaptive mechanism, which is a result of *social learning*. Social learning occurs when individuals adapt to new behavior or information regarding their environment by observing and interacting with other species [34]. The authors in [35] demonstrate that locally adaptive ecological behavior from experienced individuals assumes to be beneficial. In our context, experienced prey  $y$  and predator density  $z$  play an important role in this regard, in which case we assume that the *learning rate*  $L = L(y, z)$  appear with those arguments. The more intakes or attacks the predator do, the more signals the experienced prey transmit. In return, this will decrease the learning duration  $L^{-1}$ .

We shall mention certain assumptions to reveal an explicit formula for  $L$ . We assume that the encounter between experienced prey and predators enhances learning, therefore  $L \sim yz$ . A constant value for  $L$  is assigned when the predator density  $z$  is known to achieve a certain threshold, say  $\eta$ . Without loss of generality, we assume that  $L = 1$  when  $z = \eta$ . The proposed biological scenario thus designates the unit time (time scale) in our model as the inexperienced prey's learning duration

when  $z = \eta$ , which could be several days. The learning rate must then decrease or increase, i.e.  $L < 1$  or  $L > 1$ , when  $z$  turns to be smaller or larger than the threshold  $\eta$ . This study considers a situation where the interspecific competition between predators and prey is so intense that an average experienced prey individual has multiple encounters with predators in one day. A number of studies have shown that maternal distress in some vertebrates caused by predator encounters affect offspring's brain, which leads to attention and learning deficits [36, 37, 38]. General anxiety, depression, and less physical activeness are among other conspicuous marginal effects. Here, we take into account some proportion of the inexperienced prey (typically infants and juveniles) being products of such intense encounters. Prominent from learning deficit and less activeness is how these individuals heavily rely on parental or alloparental guard against predator's attacks. We thus impose an assumption based on this reliance that the learning rate  $L$  decreases only slowly when more parents and alloparents are present but predators are scarce, i.e. when  $y$  increases and  $z < \eta$ , and increases only slowly when  $y$  increases but the predators are overwhelming  $z > \eta$ . The latter stems from high urgency in mastering the escaping technique, adding external trigger to learning. Based on the previous descriptions, we take the following ansatz from several possibilities in forming rational functions due to its small number of parameters used:

$$L(y, z) := \frac{\alpha + yz}{\alpha + \eta y}. \quad (4)$$

We assume that both  $\alpha$  and  $\eta$  are positive. Since there is no clear indicator whether a certain age is deemed ready for learning, we immerse the age transition term for the inexperienced prey to the learning rate. Realistically, the carrying capacity  $C$  is defined in such a way that  $x, y \leq C$ , making  $L(y, z) \geq L(C, 0) > 0$  for all nonnegative  $y, z$  and that learning and age transition are unstoppable natural components of prey population.

## 2.5 Predator population growth model

In this study, we assume that there is no other food resources to maintain predators' survival except the prey. This means in the absence of prey, predators are subject to starvation and their numbers are expected to decline exponentially

$$z' = -\theta z.$$

In the presence of prey, however, this decline is opposed by birth of predators as a function of prey abundance. In the classical predator-prey models, the number of newborns is usually assumed to be proportional to the biomass resulted from predation

$$z' = \delta \cdot \frac{\beta x}{1 + \beta \tau x} \cdot z + \delta \cdot \rho \cdot \frac{\beta y}{1 + \beta \tau y} \cdot z - \theta z. \quad (5)$$

Here,  $\delta$  represents an assimilation efficiency, i.e. the efficiency of predator in converting prey biomass into offsprings.

## 3 Predator-prey model highlighting honest signals, cues and learning

### 3.1 Model summary and scaling

The ideas of the previous discussions can now be assembled to form a set of three differential equations that describe the biological dynamics of a two-species predator-prey model

$$\begin{aligned} x' &= r(x + y) - \frac{r}{C}x(x + y) - \frac{\beta x}{1 + \beta \tau x} \cdot z - \frac{\alpha + yz}{\alpha + \eta y} \cdot x, \\ y' &= \frac{\alpha + yz}{\alpha + \eta y} \cdot x - \frac{r}{C}y(x + y) - \rho \cdot \frac{\beta y}{1 + \beta \tau y} \cdot z, \\ z' &= \delta \cdot \frac{\beta x}{1 + \beta \tau x} \cdot z + \delta \cdot \rho \cdot \frac{\beta y}{1 + \beta \tau y} \cdot z - \theta z. \end{aligned} \quad (6)$$

Having a system of eleven parameters, we will first consider suitable parameters and variable transformations in order to reduce the model complexity, without affecting the main biological features. Let us introduce the scaling parameters  $X, Y, Z$  and dimensionless variables based on the scaling,  $\tilde{x} := x/X$ ,  $\tilde{y} := y/Y$ , and  $\tilde{z} := z/Z$ . We also foresee by the formulation of the learning rate that the parameter  $\alpha$  might not be measurable, i.e. unobservable. Additional to the time scaling, we suppose that  $X, Y, Z$  and  $\alpha$  are chosen in such a way that  $\sqrt{\alpha} = \eta = X = Y = Z$ . Therefore, the central of the scaling is the observable (specifiable) threshold  $\eta$ . We acquire a modification (6) as follows

$$\begin{aligned}\tilde{x}' &= r(\tilde{x} + \tilde{y}) - \frac{rX}{C}\tilde{x}(\tilde{x} + \tilde{y}) - \frac{\beta X \tilde{x}}{1 + \beta X \tau \tilde{x}} \cdot \tilde{z} - \frac{(\alpha + X^2 \tilde{y} \tilde{z})}{\alpha + X^2 \tilde{y}} \cdot \tilde{x}, \\ \tilde{y}' &= \frac{(\alpha + X^2 \tilde{y} \tilde{z})}{\alpha + X^2 \tilde{y}} \cdot \tilde{x} - \frac{rX}{C}\tilde{y}(\tilde{x} + \tilde{y}) - \rho \cdot \frac{\beta X \tilde{y}}{1 + \beta X \tau \tilde{y}} \cdot \tilde{z}, \\ \tilde{z}' &= \delta \cdot \frac{\beta X \tilde{x}}{1 + \beta X \tau \tilde{x}} \cdot \tilde{z} + \delta \cdot \rho \cdot \frac{\beta X \tilde{y}}{1 + \beta X \tau \tilde{y}} \cdot \tilde{z} - \theta \tilde{z}.\end{aligned}$$

To avoid hulking notation in the above system, we backtrack to the original variables and parameters only for simplicity. In other words,  $x \leftarrow \tilde{x}$ ,  $y \leftarrow \tilde{y}$ ,  $z \leftarrow \tilde{z}$ . Additional to this, we suppose that  $\beta \leftarrow \beta X$  and  $K := rX/C$ . The resulting simplified model which we primarily focus in the sequel can now be read as follows

$$\begin{aligned}x' &= r(x + y) - Kx(x + y) - \frac{\beta x}{1 + \beta \tau x} \cdot z - \frac{1 + yz}{1 + y} \cdot x, \\ y' &= \frac{1 + yz}{1 + y} \cdot x - Ky(x + y) - \rho \cdot \frac{\beta y}{1 + \beta \tau y} \cdot z, \\ z' &= \delta \cdot \frac{\beta x}{1 + \beta \tau x} \cdot z + \delta \cdot \rho \cdot \frac{\beta y}{1 + \beta \tau y} \cdot z - \theta z.\end{aligned}\tag{7}$$

### 3.2 Parameter ranges

Here, we assume that  $r \in [0, 1]$  and  $C \gg 1$ . Ideally, the threshold for the predator density  $\eta$  to actuate the intensive learning holds  $\eta \ll C$ , facilitating the abundance of prey. Therefore, we come into the specification  $K \in [0, 1]$ . The unobservability of the search rate (scanning speed)  $\beta$  also hints that the new  $\beta \leftarrow \beta X$  lives in  $\mathbb{R}_+$ , which depends on the type of predator considered. Recall from the model that  $\tau \ll T$ , from which when the time scale and  $T$  are comparable, we can assume  $\tau \in [0, 1]$ . We also have as previously discussed that  $\rho \in [0, 1]$ . Certain predators, e.g. snakes, can lay eggs more than the number of prey individuals (e.g. frogs) eaten in one time scale. Others like lions produce much fewer offspring as compared to the number of captured prey individuals. This study considers the later type of predator where  $\delta \in [0, 1]$ . Finally, the predator lifespan duration  $\theta^{-1}$  is assumed to be greater than the learning duration of inexperienced prey when the threshold condition holds  $z = \eta$ , therefore  $\theta \in [0, 1]$ .

### 3.3 Equilibria

Let us suppose that all the parameter values in the system (7) are positive. The system exhibits two analytically presentable equilibria:

$$\begin{aligned}E_1 &= (0, 0, 0) \quad (\text{extinction equilibrium}), \\ E_2 &= (x_2, y_2, 0) \quad (\text{predator extinction equilibrium}),\end{aligned}$$

where

$$x_2 := (y_2 r + r)y_2 \quad \text{and} \quad y_2 := \frac{\sqrt{(K + Kr)^2 + 4Kr^2} - (K + Kr)}{2Kr}.$$

For further use and brevity, let us denote by

$$(f, g, h), \quad w \in \{\beta, \delta, K, r, \rho\}, \quad \arg_w \ell(w)$$

the vector field in the system (7), a representative of the chosen bifurcation parameters, and positive solution(s)  $w$  such that  $\ell(w) = 0$ , respectively. In the forthcoming study of codim-1 bifurcations, we assume to have fixed other parameter values once  $w$  is chosen.

The first finding regarding  $E_1$  reveals that the Jacobian matrix  $\nabla_{(x,y,z)}(f, g, h)|_{E_1}$  has the eigenvalues  $-1, r, -\theta$ . This means that the system has a one-dimensional unstable manifold and a two-dimensional stable manifold around  $E_1$ . In other words,  $E_1$  has the configuration of a saddle node. Moreover, any value of  $w$  forming a concatenated point  $(w, E_1)$  cannot be a bifurcation point (branching point) due to non-singularity of the Jacobian matrix, see Crandall and Rabinowitz [39].

As far as  $E_2$  is concerned, the following results are expected. The block matrix  $\nabla_{(x,y)}(f, g)|_{E_2}$  has eigenvalues  $-r, -2r\sqrt{(K+Kr)^2+4Kr^2}/(\sqrt{(K+Kr)^2+4Kr^2}-K+Kr)$ . Furthermore, the full Jacobian matrix has zero entries on the third row except on the diagonal, whose entry is given by

$$\lambda_0 := \frac{\delta\beta x_2}{1+\beta\tau x_2} + \frac{\delta\rho\beta y_2}{1+\beta\tau y_2} - \theta. \quad (8)$$

This reveals that the model (7) has a stable manifold around  $E_2$  of dimension at least 2. We also know that any value of  $w$  concatenated with  $E_2$  cannot form a branching point except  $(\arg_w \lambda_0, E_2)$ , providing  $\arg_w \lambda_0$  exists, because the Jacobian matrix is singular at the point. Let us suppose that certain numerical values for all parameters except  $w$  are given such that  $\arg_w \lambda_0$  exists. Our next aim is to confirm that  $(\arg_w \lambda_0, E_2)$  is indeed a branching point and a continuum of nontrivial (coexistence) equilibria bifurcates from the point under perturbation of  $w$  around  $\arg_w \lambda_0$ . We argue that direct substitutions and solving a higher-order polynomial of either of the three state variables returns complications, in which case we favor the aid of bifurcation theory. The analysis centers on the behavior of the equilibrium due to perturbation of  $w$  when the equilibrium is sufficiently close to  $E_2$ .

The vector field  $(f, g)$  generates a system of algebraic equations where  $x$  and  $y$  change as a response of perturbation of  $z$ . We know that in some subset of  $\mathbb{R}^3$  where  $x, y$  are nonnegative, the vector field  $(f, g)$  is  $C^\infty$ . According to Implicit Function Theorem, the nonsingularity of the block matrix  $\nabla_{(x,y)}(f, g)|_{E_2}$  gives neighborhoods  $U(x_2, y_2)$  of  $(x, y)$  and  $V(0)$  of  $z$  where  $(x, y) = (x(z), y(z)) \in C^\infty(V(0))$  solves the equilibrium equation  $(f, g) = 0$  for any given  $z \in V(0)$  and  $\lim_{z \rightarrow 0}(x, y) = (x_2, y_2)$  in the neighborhood  $U(x_2, y_2)$ . For further use, let us define

$$M := \left\| \nabla_{(x,y)}^{-1}(f, g) \cdot \begin{pmatrix} \partial_z f \\ \partial_z g \end{pmatrix} \right\|_{L^\infty(U(x_2, y_2), V(0))}$$

that specifies a Lipschitz constant of  $x(z)$  and  $y(z)$ , i.e.

$$|x - x_2| \leq M|z| \quad \text{and} \quad |y - y_2| \leq M|z| \quad (9)$$

for all  $z \in V(0)$ . The Implicit Function Theorem helps guarantee that  $M$ , which contains the evaluated right-hand sides of  $x'(z)$  and  $y'(z)$  on the neighborhoods, exists and is bounded. The yet untreated equilibrium equation  $h = 0$  from (7) can now be rearranged via Taylor expansions of  $\beta x/(1+\beta\tau x)$  around  $x_2$  and  $\beta y/(1+\beta\tau y)$  around  $y_2$  and (9) into the *canonical form* of bifurcation equation

$$h(z) = \lambda_0 z - \lambda z + \omega(z) = 0, \quad \text{where } \lambda = 0, \omega(z) = \mathcal{O}(|z|^2) \text{ as } z \rightarrow 0 \quad (10)$$

and  $\lambda_0$  is as given in (8). Apparently, the equation (10) resembles the Lyapunov-Schmidt reduced form [40, 41]. When a small positive  $z$  is shown to solve (10), the continuity of  $x(z)$  and  $y(z)$  guarantees the existence of a coexistence equilibrium. Our next aim is thus to synthesize conditions from the canonical form (10) under which a positive  $z$  bifurcates from 0. Work on analyzing such canonical form has been ubiquitous, which typically includes Brouwer Degree Theory, Brouwer Index Theory, and Rabinowitz's Global Bifurcation Theorem. However, it is not our aim in this paper to recall the exhaustive content of the theories. Despite instantly picking up corresponding terminologies, we will place the accompanying references for further reading, whenever necessary.

Consider the canonical form (10) where  $h : Q \rightarrow \mathbb{R}$  for some open interval  $Q \subset \mathbb{R}$  and  $h \in C^\infty(Q)$ . A point  $s \in \mathbb{R}$  where  $s \notin h(\partial Q)$  is called *regular* if either  $h^{-1}(s) = \emptyset$  or all points  $z^* \in h^{-1}(s)$  make



$h'(z^*)$  invertible, otherwise it is called *critical*. The map  $\mathcal{B} : C^1(Q) \times Q \times \mathbb{R} \rightarrow \mathbb{Z}$  defined as

$$\mathcal{B}(h, Q, s) := \begin{cases} \sum_{z^* \in h^{-1}(s)} \text{sign}(h'(z^*)), & s \text{ regular,} \\ \mathcal{B}(h, Q, \tilde{s}), & s \text{ critical, } \tilde{s} \text{ regular, with } \|s - \tilde{s}\| < \inf_{m \in h(\partial Q)} \|s - m\|, \end{cases}$$

denotes the *Brouwer degree* of  $h$  in an interval  $Q$  with respect to a reference point  $s$  [42, 43]. When  $z = 0$  is an isolated singular value of  $h$  (i.e. no further singular value of  $h$  in a certain neighborhood  $Q(0)$  of 0), then the map

$$\mathcal{I}(h, 0) := \mathcal{B}(h, Q(0), 0)$$

defines the *index* of  $h$  at the isolated singular value  $z = 0$ , which is derived from Brouwer degree of  $h$  in a neighborhood of  $z = 0$  with respect to the reference point  $s = 0$ . At this stage, we know that whether  $z = 0$  is isolated or not depends on the neighbourhood  $Q(0)$  taken. Confirming that  $(\arg_w \lambda_0, 0)$  is a branch point of (10) requires that the index changes in value when  $w$  is perturbed around  $\arg_w \lambda_0$  [42]. Let us thus suppose that  $0 = \lambda \neq \lambda_0$  such that the polynomial  $h$  in (10) has a nonzero slope at  $z = 0$  (i.e.  $h'(0) = \lambda_0 - \lambda \neq 0$ ) and choose  $Q(0)$  sufficiently small such that  $h^{-1}(0) = \{0\}$ . The former indicates that  $z = 0$  is an isolated singular value and  $s = 0$  is regular. The index is then given by

$$\mathcal{I}(h, 0) = \text{sign}(h'(0)) = \text{sign}(\lambda_0 - \lambda) = \begin{cases} 1, & \lambda_0 > \lambda = 0 \\ -1, & \lambda_0 < \lambda = 0 \end{cases}.$$

This claims that  $(\arg_w \lambda_0, 0)$  is indeed a branching point of (10). Let us suppose that

$$w > \arg_w \lambda_0 \Leftrightarrow \lambda_0 > 0.$$

One can pick an example to this case for suitable numerical values when  $\lambda_0$  changes from negative to positive as  $\beta$  increases. Suppose that  $\lambda_0 \neq \lambda = 0$ , further rearrangement of (10) into

$$z - \lambda \mathcal{L}z + \tilde{\omega}(z) = 0, \text{ where } \mathcal{L} := \lambda_0^{-1}, \tilde{\omega}(z) = \mathcal{L}\omega(z) = \mathcal{O}(|z|^2) \text{ as } z \rightarrow 0,$$

fits into the framework in [44, pp. 161–166] and [45], where the eigenvector corresponding to the largest eigenvalue of  $\mathcal{L}$  gives the leading order (initial direction) of the continuum of bifurcating positive solutions, according to the representation

$$z = \text{eigvec}\{\mathcal{L}\} \cdot \varepsilon + \mathcal{O}(\varepsilon^2)$$

for a sufficiently small  $\varepsilon > 0$ . In our current study, the condition

$$w > \arg_w \lambda_0 \tag{11}$$

shall give  $\mathcal{L} = \lambda_0^{-1} > 0$ . According to the aforementioned references, a continuum of positive solutions  $z$  to (10) bifurcates from  $(\arg_w \lambda_0, 0)$  with the note that  $w$  is sufficiently close to  $\arg_w \lambda_0$ .

As the reminder, we note that the preceding exposition solely scopes out the behavior of equilibrium around a branching point and the existence of a branching continuum of coexistence equilibria around the point, excluding the uniqueness. To go beyond both cases, we perform a numerical bifurcation analysis employing all the aforementioned bifurcation parameters in the next section.

## 4 Numerical study of the predator-prey model via path-following methods

In this section, our main concern will be to investigate the dynamical response of the predator-prey system (7) as certain model parameters are varied. Specifically, we will take the predator's search rate  $\beta$ , the predator's assimilation efficiency  $\delta$ , the intrinsic growth rate of prey  $r$ , the competition coefficient  $K$  and the separator  $\rho$  as our main bifurcation parameters. The numerical investigation will be carried out using the path-following software COCO (short form of Computational Continuation Core [46]). This is an analysis and development platform for the numerical treatment of continuation



problems using MATLAB. A remarkable feature of COCO is its set of toolboxes that covers, to a good extent, the functionality of available continuation packages, such as AUTO [47] and MATCONT [48]. In particular, in this section we will make extensive use of the COCO-toolboxes ‘ep’ and ‘po’, which encompass a set of routines for the bifurcation analysis of parameter-dependent families of equilibria and limit cycles, respectively, in smooth dynamical systems.

Parameter	Description	Unit	Range	Reference value
$r$	Prey’s intrinsic growth rate	$[\text{t}^{-1}]$	0–1	0.8
$K$	Competition coefficient	$[\text{t}^{-1}]$	0–1	0.1
$\beta$	Scaled predator’s search rate	$[\text{a} \times \text{ind} \times \text{t}^{-1}]$	0–3	1.7
$\tau$	Predator’s handling time	$[\text{t}]$	0–1	0.3
$\rho$	Separator between honest signal and cue	–	0–1	0.5
$\delta$	Predator’s assimilation efficiency	–	0–1	0.7
$\theta$	Predator’s natural death rate	$[\text{t}^{-1}]$	0–1	0.1

Table 1: Parameter values used for the numerical bifurcation analysis. The unit symbol t, a, ind stand for unit time, unit area, and individual, respectively.

Let us begin our study by analyzing the behavior of the equilibria of the model (7) as the predator’s search rate  $\beta$  and the predator’s assimilation efficiency  $\delta$  vary, one at the time. The result can be observed in Fig. 1. In the figure, the blue and red curves represent continuation of coexistence and predator extinction equilibria, respectively. Panel (a) reveals that for small values of  $\beta$  the system possesses a stable predator extinction equilibrium, meaning that under this condition any initial predator population will decay in time. As  $\beta$  increases, a critical value  $\beta = \arg_{\beta} \lambda_0 \approx 0.02144$  (labeled BP1) is detected, where the predator extinction equilibrium loses stability. From this point on, another branch (in blue) emerges, corresponding to the numerical continuation of stable coexistence equilibria, where the predator population can now be sustained. This abrupt change in the system behavior corresponds to a branching point (of supercritical type) [49, 50], also known in the Mathematical Biology field as a forward bifurcation [51, 52]. For  $\beta$  larger than this branching point, a maximal value of the predator population size (under equilibrium) is found at  $\beta \approx 0.07049$ . This value can be interpreted as the optimal predator’s search rate, in the sense that smaller  $\beta$  means the predator population is not taking advantage of the available food source provided by the prey, while  $\beta$  too high means a faster decrease of the prey population, making the predator’s food source scarce. Another critical point is found at  $\beta \approx 1.62824$ , where a supercritical Hopf bifurcation H1 takes place, hence giving rise to a family of stable limit cycles, while the equilibrium becomes unstable. A similar scenario occurs when the predator assimilation efficiency  $\delta$  is varied, see Fig. 1(b). In this case, as before, small  $\delta$  makes the predator population unsustainable in the system, until the critical value  $\delta = \arg_{\delta} \lambda_0 \approx 0.02963$  is reached, where the system undergoes another forward bifurcation (BP2). For larger values, the bifurcation analysis reveals the presence of a family of limit cycles, limited by two Hopf points (H2 at  $\delta \approx 0.07964$ , H3 at  $\delta \approx 0.75458$ ), hence defining a window of sustained oscillations with amplitudes strongly dependent on the predator’s assimilation efficiency  $\delta$ . Thus, the system presents a branch of stable oscillatory behavior forming a closed loop, starting and ending at the Hopf points H2 and H3, see Fig. 1(c). This dynamical phenomenon is referred often to as *endemic bubble* [53].

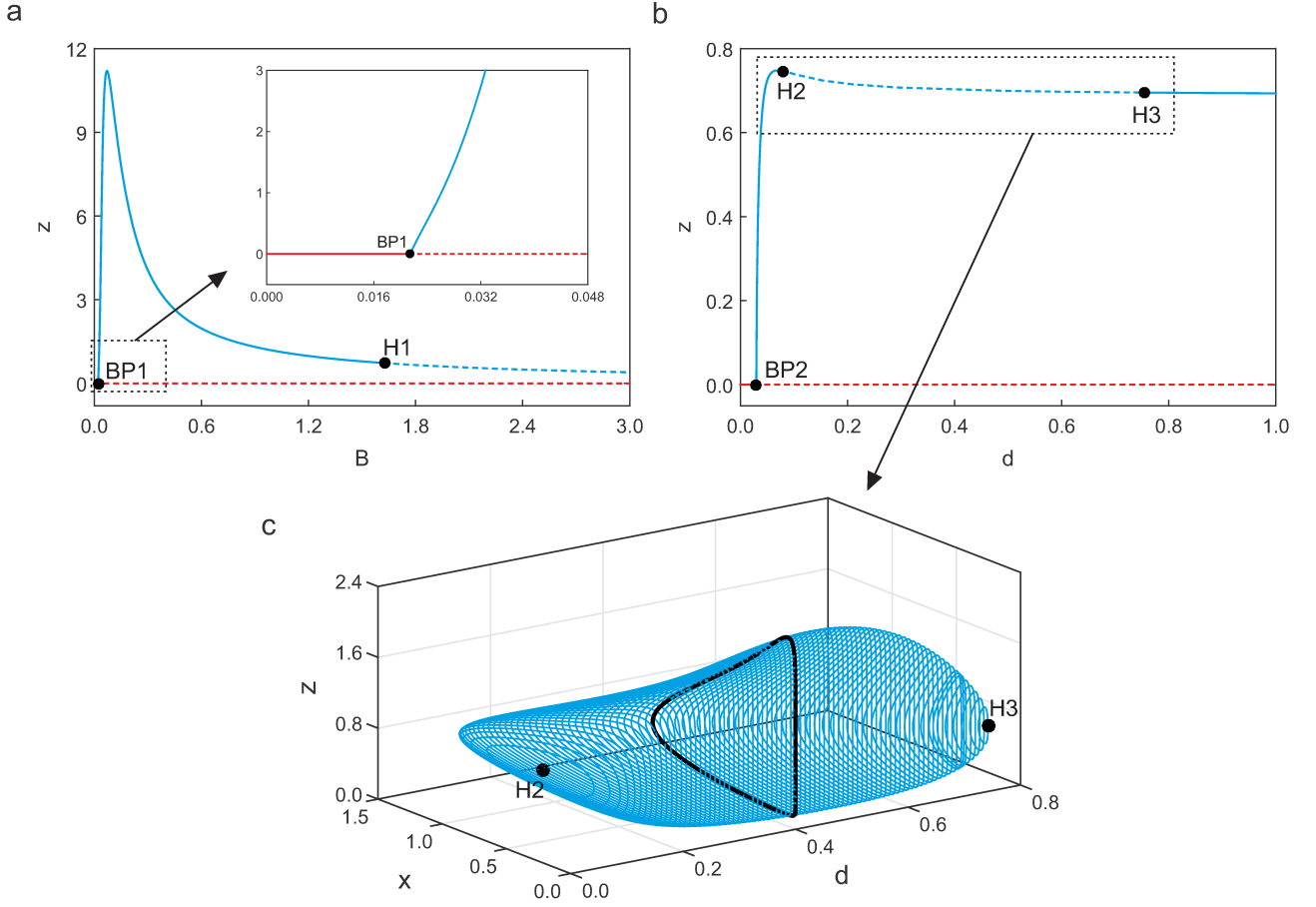


Figure 1: One-parameter continuation of equilibria of system (7) with respect to the predator’s search rate  $\beta$  (panel (a)) and the predator’s assimilation efficiency  $\delta$  (panel (b)), computed for the parameter values given in Table 1. In these panels, the blue and red curves represent continuation of endemic and predator-free equilibria, respectively. Solid and dashed lines depict stable and unstable solutions, respectively. Bifurcation points are highlighted as follows:  $BP_i$  (branching points) and  $H_i$  (Hopf points). Panel (c) shows the solution manifold obtained via continuation of periodic solutions between the Hopf points  $H2$  and  $H3$  found in panel (b). The figure shows a cross section corresponding to a periodic solution at  $\delta = 0.4$ .

Next, we will analyze in more detail the periodic response of the predator-prey model considered here. For this purpose, we will fix all parameter values according to Table 1 and let the predator search rate  $\beta$  vary for  $\beta > 1.62824$ , that is, after the Hopf bifurcation at  $H1$  occurs. The result of the numerical continuation of the parameter-dependent family of periodic solutions is shown in Fig. 2. Panel (a) shows the behavior of the mean value of the  $z$ -component of the periodic response as  $\beta$  varies. Panel (b) depicts the family of periodic orbits on the  $x$ - $y$  plane. This figure suggests that the sequence of limit cycles converges to a homoclinic solution, i.e., a trajectory that approaches a saddle equilibrium for  $t \rightarrow \pm\infty$ . Typical state-space representations of near-homoclinic orbits are characterized by the development of a “corner” in the phase-plot located close to the saddle-equilibrium, as can be detected in Fig. 2(b), while the period of the limit cycles increases showing long excursions around the equilibrium (in this case the extinction equilibrium  $x = y = z = 0$ ) due to the slow dynamics. Biologically speaking, this means that the predator and prey populations present fluctuations with episodes of almost-extinction of long duration. The oscillatory behavior indicates that the ecosystem provides suitable conditions for all populations to recover again after the near-extinction phase. At the homoclinic solution, however, the three populations can experience only one phase of growing behavior after which all populations go extinct. In other words, only one generation can be sustained by the ecosystem, see Fig. 3(c)–(e).

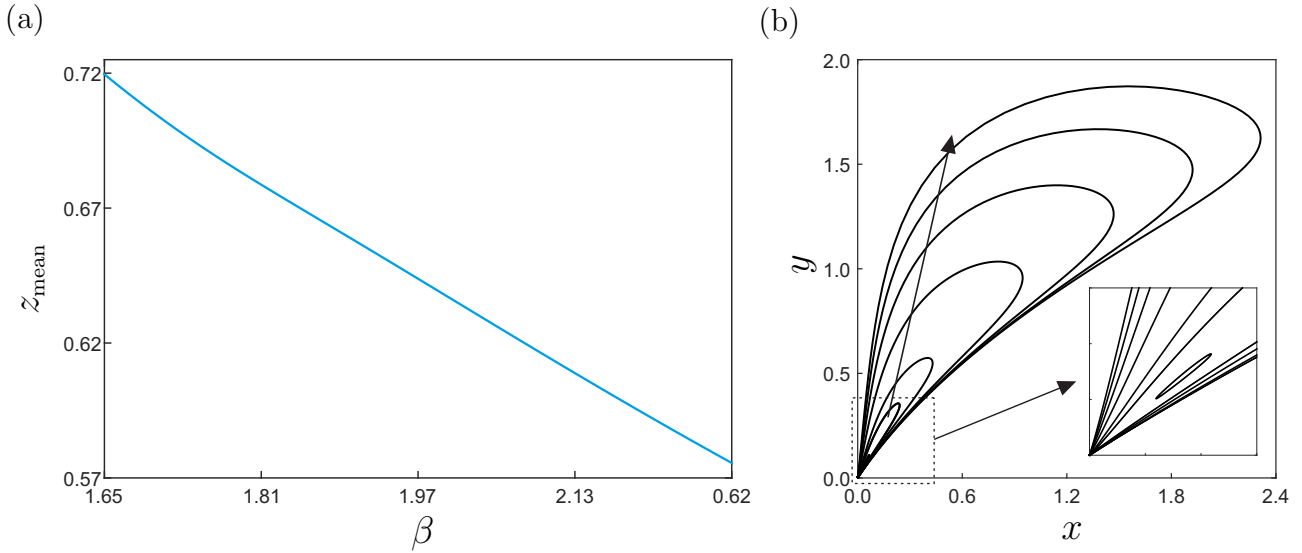


Figure 2: (a) One-parameter continuation of periodic solutions of system (7) with respect to the predator's search rate  $\beta$ , computed for the parameter values given in Table 1. In this panel, the vertical axis shows the mean value of the  $z$ -component of the periodic response. Panel (b) depicts a sequence of closed orbits obtained along the curve shown in panel (a). Here, the direction of increasing  $\beta$  is indicated by an arrow.

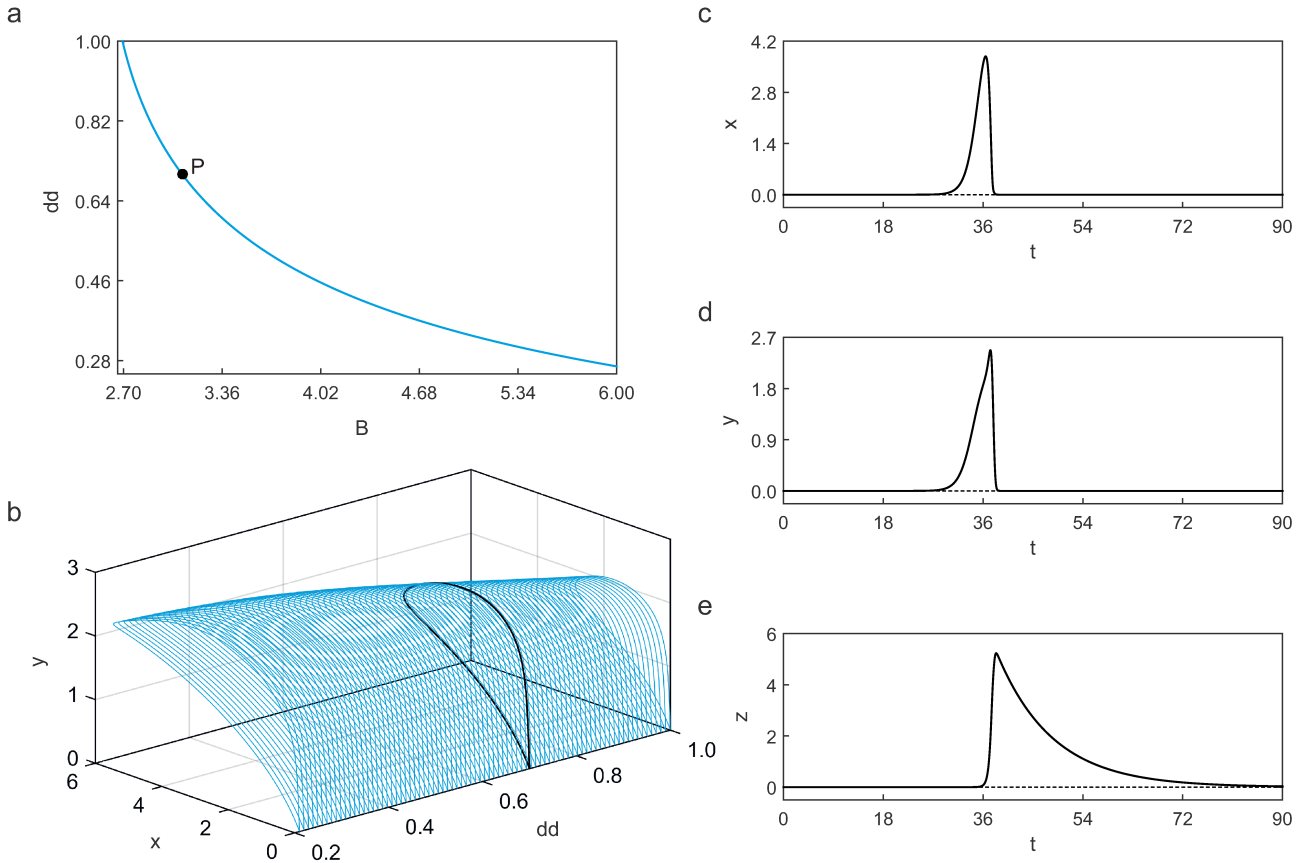


Figure 3: (a) Two-parameter continuation of a family of periodic solutions with high period approximating a homoclinic orbit, with respect to  $\beta$  and  $\delta$ , for the parameter values given in Table 1. Panels (c)–(e) present time plots of a solution computed at the test point P ( $\beta = 3.0918$ ,  $\delta = 0.7$ ). Panel (b) depicts the solution manifold computed along the curve in panel (a), showing a cross section corresponding to the test solution found at P.

As is well known, a family of near-homoclinic orbits can be computed via numerical continuation of

periodic solutions with large (fixed) period [46], as a homoclinic solution can be found as the limit of a branch of periodic orbits when the period tends to infinity, connecting a saddle equilibrium with itself. In this way, we will compute a branch of near-homoclinic orbits when the predator search rate  $\beta$  and the predator assimilation efficiency  $\delta$  vary simultaneously, see Fig. 3(a). Thus, we obtain an approximation of a family of  $(\beta, \delta)$ -values where periodic solutions disappear via a homoclinic bifurcation. Panel (b) depicts the solution manifold projected on the  $x$ - $y$  plane along the near-homoclinic curve. Here, it can be seen that all solutions have the extinction equilibrium as the base point. Panels (c)–(e) present the time profiles of all populations showing the rise and decay phases described in the previous paragraph.

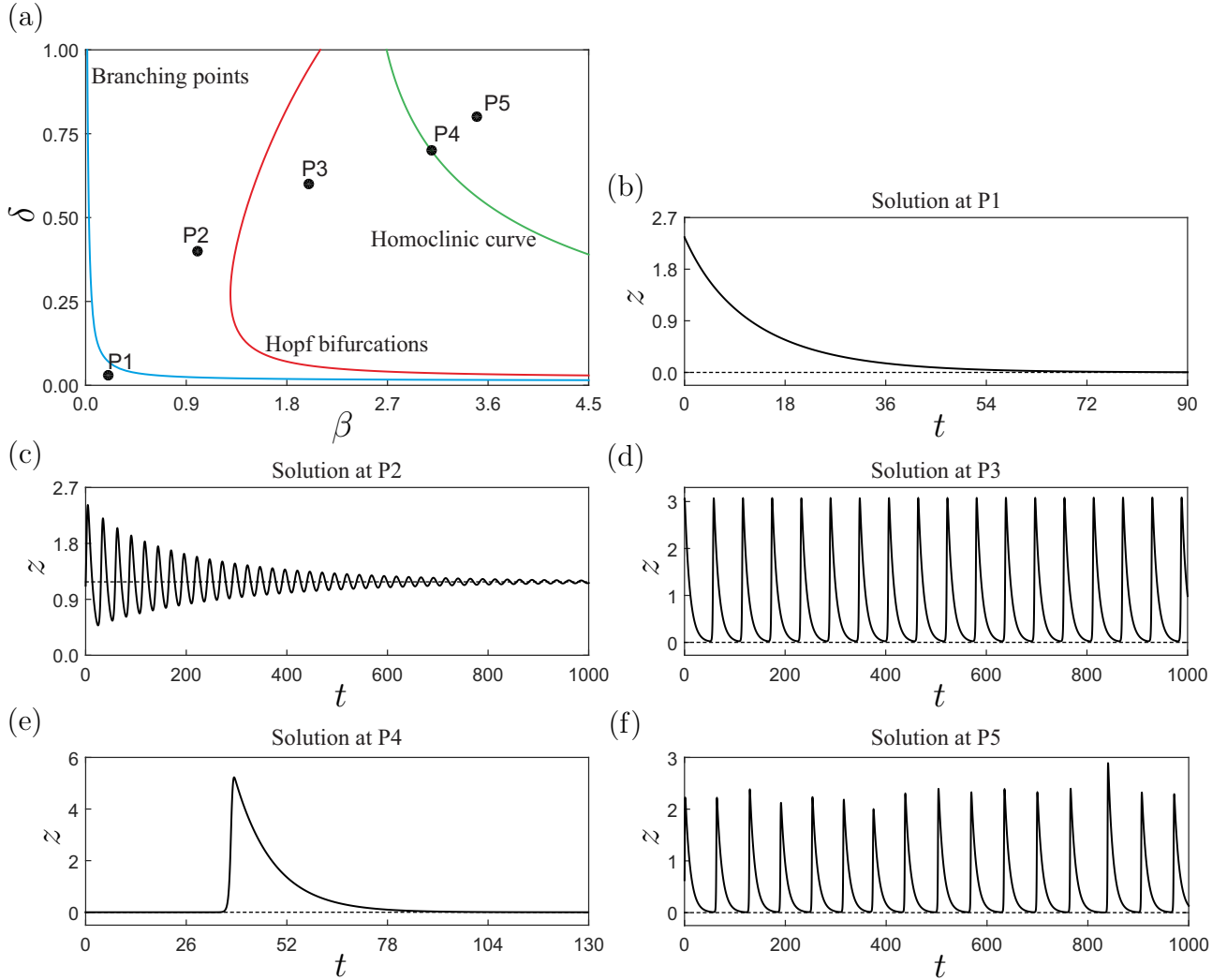


Figure 4: (a) Two-parameter continuation with respect to  $\beta$  and  $\delta$  of the codimension-1 bifurcations BP1 (in blue) and H1 (in red, see Fig. 1(a)), together with the homoclinic curve computed in Fig. 3 (in green). Panels (b)–(f) show time plots corresponding to the test points P1 ( $\beta = 0.2, \delta = 0.03$ ), P2 ( $\beta = 1, \delta = 0.4$ ), P3 ( $\beta = 2, \delta = 0.6$ ), P4 ( $\beta = 3.0918, \delta = 0.7$ ) and P5 ( $\beta = 3.5, \delta = 0.8$ ).

Our numerical investigation has revealed the presence of two local and one global bifurcation in the predator-prey model (7), which are responsible for significant changes in the system response under parameter variations. In our study, we are considering the predator’s features (search rate and assimilation efficiency) as the parameters of interest and we will investigate how the system dynamics can be classified according to those features. For this purpose, we will use COCO’s capability to carry out the numerical continuation of codimension-1 bifurcations when two parameters are varied simultaneously. Specifically, we will perform the numerical continuation of the bifurcation points H1 and BP1 found in Fig. 1(a) and the homoclinic bifurcation, with respect to the parameters of interest  $\beta$  and  $\delta$ . The result can be seen in Fig. 4(a). This figure presents three curves corresponding to the continuation of the bifurcation points mentioned before. The lowest curve (in blue) represents

$(\beta, \delta)$ -tuples producing branching points. In this way, the curve divides locally the parameter space into two regions: one for which the predator is present in the ecosystem, and one where the predator population disappears. The curve indicates that to ensure the predator's survival, a low assimilation efficiency has to be compensated with a high search rate and vice versa. A second curve (plotted in red) represents the numerical continuation of the Hopf point H1 mentioned before. This curve then defines a boundary for the appearance of endemic periodic solutions, where all populations coexist in the ecosystem following an oscillatory pattern. Finally, the third curve (in green) represents the numerical continuation of near-homoclinic orbits described previously, which gives an approximation of a curve of homoclinic bifurcations. Crossing this curve from below destroys periodic solutions via this global bifurcation, while all equilibria of the system (extinction, predator extinction and coexistence) are unstable. Further numerical investigation reveals the presence of quasi-periodic orbits, as can be seen in Fig. 4(f). In this figure, panels (b)–(f) show time profiles corresponding to an excursion across the two-parameter bifurcation diagram in panel (a).

To conclude our investigation, we will now consider the system dynamics under parameter variations related to the prey's characteristics. Specifically, we will carry out a two-parameter continuation of the codimension-1 bifurcations found before (branching point, Hopf, homoclinic) with respect to the prey's intrinsic growth rate  $r$  and the competition coefficient  $K$ . The result can be seen in Fig. 5(a). Similar to Fig. 4(a), this diagram shows three curves representing  $(r, K)$ -values producing the codimension-1 bifurcations specified above. The resulting curves reveal that in the considered biological scenario, the predator population enjoys strong survival possibilities, as the region for which the predators disappear is very narrow (the area between the vertical axis and the blue curve corresponding to branching points). This means that only significantly low prey's intrinsic growth rates would endanger the predator sustainability in the system. A similar scenario is encountered if we now take the prey's intrinsic growth rate  $r$  and the predation reduction coefficient  $\rho$ , see Fig. 5(b). As before, the curves depicted in this diagram allows the classification of the model behavior according to the considered parameters corresponding to the prey's features.

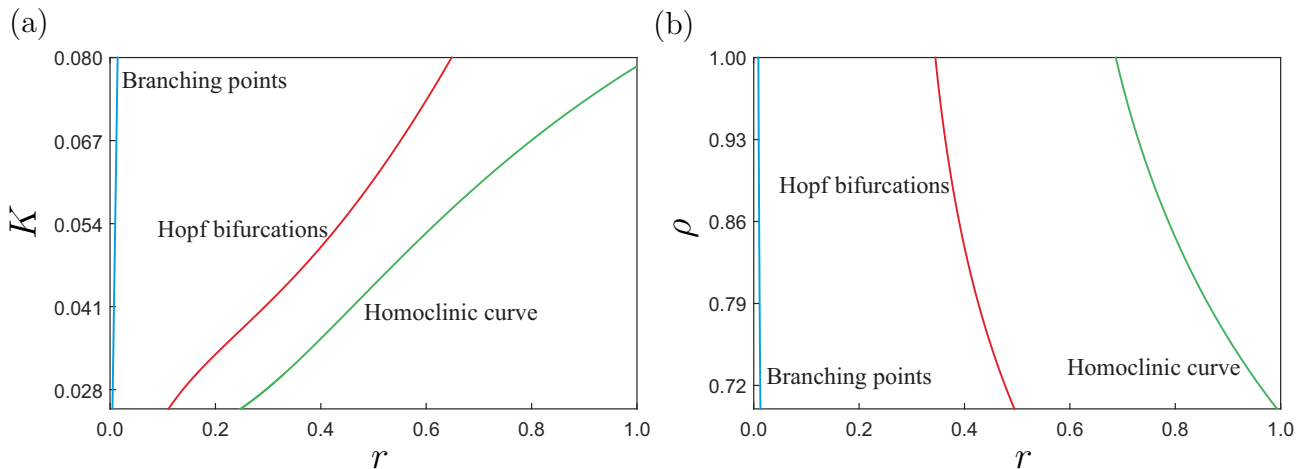


Figure 5: Two-parameter continuation of branching points (in blue), Hopf bifurcations (in red) and homoclinic orbits (in green), with respect to  $(r, K)$  (panel (a)) and  $(r, \rho)$  (panel (b)), computed for the parameter values given in Table 1. The color code is as in Fig. 4(a).

## 5 Discussion and concluding remarks

In the present work, we propose a three-stage, two-species predator-prey model that incorporates the role of honest signals and cues. We subdivide the prey population into the subpopulation of inexperienced individuals that are not able to transmit honest signals (typically infants and juveniles) and that of experienced individuals that are able to do so. Unlike the widely-used game-theoretic models, our model focuses on the effect of honest signals, cues and the associated learning among inexperienced individuals to shape their genetically-inherited anti-predation technique on the population level. The standard birth term, logistic competition term, and predation term inspired by Holling's time bud-

getting principle are involved in the model. A border line between honest signal and cue is controlled by the parameter  $\rho$ . The value of  $\rho$  close to 0 indicates that the average experienced prey individual successfully transmit signals and they are digested as honest signals by all the nearby predators, such that no catch will be pursued against it. This condition emphasizes the presence of what we call error-free honest signals. When  $\rho$  is close to 1, then some predators accept the transmitted signals as honest, but some others do not (maybe those in distant ranges) and such flawed honest signals even help the latter locate the whereabouts of the prey individual. The flawed honest signals, when benefitting the predators exclusively, turn into cues. We further model a learning rate for the inexperienced prey conveying the information regarding different learning speeds when the predator density is around a certain threshold  $\eta$ . Below the threshold, the learning rate (speed) is relatively small (smaller than one) and decreases only slowly as the experienced prey tends to be more abundant, that is, due to overwhelming parental protection. Above the threshold, the learning rate is relatively large and increases slowly with the experienced prey density, also due to parental protection. For the sake of simplification, we further performed a scaling of the original model with eleven parameters to obtain that with seven parameters. Buckingham  $\pi$ -Theorem suggests that the eleven parameters can be cut to the least of eight parameters using dimensional analysis, otherwise biological questions arise. In our case, imposing  $\sqrt{\alpha} = \eta$  in the learning rate due to the non-observability of  $\alpha$  is a stringent assumption. Even though the case might be representable by a certain prey type in some approximation, finding the exact types that fall into the equality can however be a hard task. Therefore, what we draw from the numerical bifurcation analysis are worth of consideration that they are applied only to this restrictive case.

We point out several biological remarks regarding the numerical bifurcation analysis. We argue from the model that a certain value for the predator's search rate  $\beta$  sets a threshold or the lower bound for the coexistence between predator and prey population. The asymptotic predator density increases for larger  $\beta$  and decreases as  $\beta$  increases further, indicating a trade-off between slow uptake, which leaves more food for population sustenance, and fast uptake, which induces food's scarcity. When  $\beta$  tends to be larger, the predator population exhibits transient cycles between persistence and near-extinction, represented by the bifurcating stable limit cycles from a Hopf point. Apparently, larger values of  $\beta$  depict typical (bounded) cycles with the period tending to blow up where the cycle ultimately collides with the saddle-node extinction equilibrium. At this stage, the predator and prey population are attracted to a homoclinic orbit and ultimately go to extinction after long time. The same algorithm can be used to reproduce the  $(\beta, \delta)$ -values at which homoclinic orbits with the extinction equilibrium as the homoclinic point occur. Our computation reveals that homoclinic orbits can be seen through relatively large values of  $\beta$  and the predator's assimilation efficiency  $\delta$ , with a conflicting mode. That is, they occur specifically when  $\beta$  and  $\delta$  cannot be independently large. Any value exceeding the tuple returns a quasi-periodic orbit where the dynamics of the predator and prey population remains cyclical. All the preceding expositions indicate the exclusiveness of the homoclinic orbits, which encounter in between cyclical dynamics under a specific set of  $(\beta, \delta)$ -values. A similar situation as for  $\beta$  also happens with  $\delta$ . A certain threshold is needed for the long-term sustenance of the predator population. Then, the asymptotic predator density increases and decreases with  $\delta$ , which shows the impact of slow and fast reproduction on the scarcity of prey. With larger values, similar transient cycles between persistence and near-extinction occur, but they fold up into asymptotic densities as  $\delta$  increases further. This nontrivial finding indicates that a stable asymptotic density of the predator individuals is expected when they produce offspring much smaller than or nearly of the same magnitude as the captured prey individuals per unit area. As far as the parameters  $K, r, \rho$  are concerned, similar arguments as before can be drawn. We found that reducing the competition coefficient  $K$  under a moderate intrinsic growth rate  $r$  (around 0.5) gives an increasing degree of complexity in the asymptotic behavior of the predator-prey dynamics. This is to say that increasing the prey carrying capacity (due to  $C \sim 1/K$ ) not only accommodates prey with enough space and food resources, but also facilitates the discovery of nontrivial trajectories: transient cycles, homoclinic orbits and quasi-periodic orbits. Unlike the  $(\beta, \delta)$ -tuple, increasing  $K$  and  $r$  simultaneously can preserve the type of orbit discovered. Further numerical finding reveals that the separator between honest signal and cue  $\rho$  is only sensitive if the intrinsic growth rate  $r$  is relatively large (above 0.6). A small  $\rho$  can

only lead the model solution to the stable asymptotic predator–prey density, meaning that when the experienced prey always bears error-free honest signals, the entire populations coexist and verge on an equilibrium after long time. When the quality of the signals is compromised by a certain fraction of hunting predators ( $\rho$  increases), the equilibrium exhibits instability, yet the stability is taken over by the bifurcating limit cycles, inducing unpredictability of the dynamics that runs around persistence and near-extinction up to a certain degree. Until then, quasi-periodic orbits dominate at sufficiently large  $\rho$  (close to 1), which add more degree of unpredictability. We thus argue from the model that error-free honest signals lead to not only a stable predator–prey dynamics but also predictable behavior.

## Acknowledgements

The second author has been supported by the DAAD Visiting Professorships programme at the University of Koblenz-Landau, Germany.

## References

- [1] M. J. Owren, D. Rendall, and M. J. Ryan, “Redefining animal signaling: influence versus information in communication,” *Biology & Philosophy*, vol. 25, no. 5, pp. 755–780, 2010.
- [2] W. J. Smith, “The behavior of communicating, after twenty years,” in *Perspectives in Ethology* (D. H. Owings, M. D. Beecher, and N. S. Thompson, eds.), Boston, MA: Springer US, 1997.
- [3] M. D. Hauser, *The evolution of communication*. Cambridge, MA: MIT press, 1996.
- [4] T. Bugnyar, M. Kijne, and K. Kotrschal, “Food calling in ravens: are yells referential signals?,” *Animal Behaviour*, vol. 61, no. 5, pp. 949–958, 2001.
- [5] K. D. Lehmann, B. W. Goldman, I. Dworkin, D. M. Bryson, and A. P. Wagner, “From cues to signals: evolution of interspecific communication via aposematism and mimicry in a predator-prey system,” *PloS one*, vol. 9, no. 3, p. e91783, 2014.
- [6] R. A. Johnstone and A. Grafen, “The continuous sir philip sidney game: a simple model of biological signalling,” *Journal of theoretical Biology*, vol. 156, no. 2, pp. 215–234, 1992.
- [7] M. Leal, “Honest signalling during prey–predator interactions in the lizard *anolis cristatellus*,” *Animal Behaviour*, vol. 58, no. 3, pp. 521–526, 1999.
- [8] A. Zahavi, “Mate selection a selection for a handicap,” *Journal of theoretical Biology*, vol. 53, no. 1, pp. 205–214, 1975.
- [9] A. Zahavi, “The cost of honesty (further remarks on the handicap principle).,” *Journal of theoretical Biology*, vol. 67, no. 3, pp. 603–605, 1977.
- [10] A. ZAHAVI, “The theory of signal selection and some of its implications,” *International Symposium of Biological Evolution, 1987*, pp. pp 305–327, 1987.
- [11] R. Dawkins and J. R. Krebs, “Animal signals: information or manipulation,” *Behavioural ecology: An evolutionary approach*, vol. 2, pp. 282–309, 1978.
- [12] J. Krebs, R. Dawkins, and N. Davies, “Behavioral ecology: An integrated approach,” 1984.
- [13] A. Zahavi and A. Zahavi, *The handicap principle: A missing piece of Darwin’s puzzle*. Oxford University Press, Oxford, UK, 1999.
- [14] A. Grafen, “Biological signals as handicaps,” *Journal of theoretical biology*, vol. 144, no. 4, pp. 517–546, 1990.



- [15] S. Számadó and D. J. Penn, “Why does costly signalling evolve? challenges with testing the handicap hypothesis,” *Animal behaviour*, vol. 110, p. e9, 2015.
- [16] C. T. Bergstrom, S. Számadó, and M. Lachmann, “Separating equilibria in continuous signalling games,” *Philosophical Transactions of the Royal Society of London. Series B: Biological Sciences*, vol. 357, no. 1427, pp. 1595–1606, 2002.
- [17] T. Getty, “Handicap signalling: when fecundity and viability do not add up,” *Animal Behaviour*, vol. 56, no. 1, pp. 127–130, 1998.
- [18] T. Getty, “Sexually selected signals are not similar to sports handicaps,” *Trends in Ecology & Evolution*, vol. 21, no. 2, pp. 83–88, 2006.
- [19] M. Lachmann, S. Szamado, and C. T. Bergstrom, “Cost and conflict in animal signals and human language,” *Proceedings of the National Academy of Sciences*, vol. 98, no. 23, pp. 13189–13194, 2001.
- [20] S. Számadó, “The cost of honesty and the fallacy of the handicap principle,” *Animal Behaviour*, vol. 81, no. 1, pp. 3–10, 2011.
- [21] T. J. Polnaszek and D. W. Stephens, “Why not lie? costs enforce honesty in an experimental signalling game,” *Proceedings of the Royal Society B: Biological Sciences*, vol. 281, no. 1774, p. 20132457, 2014.
- [22] S. M. Clifton, R. I. Braun, and D. M. Abrams, “Handicap principle implies emergence of dimorphic ornaments,” *Proceedings of the Royal Society B: Biological Sciences*, vol. 283, no. 1843, p. 20161970, 2016.
- [23] O. Hasson, “Towards a general theory of biological signaling,” *Journal of Theoretical Biology*, vol. 185, no. 2, pp. 139–156, 1997.
- [24] R. A. Johnstone and A. Grafen, “Error-prone signalling,” *Proceedings of the Royal Society of London. Series B: Biological Sciences*, vol. 248, no. 1323, pp. 229–233, 1992.
- [25] R. A. Johnstone, “Honest signalling, perceptual error and the evolution of ‘all-or-nothing’ displays,” *Proceedings of the Royal Society of London. Series B: Biological Sciences*, vol. 256, no. 1346, pp. 169–175, 1994.
- [26] J. M. Smith and D. Harper, *Animal signals*. Oxford University Press, Oxford, UK, 2003.
- [27] M. E. Laidre and R. A. Johnstone, “Animal signals,” *Current Biology*, vol. 23, no. 18, pp. R829–R833, 2013.
- [28] D. Rendall, M. J. Owren, and M. J. Ryan, “What do animal signals mean?,” *Animal Behaviour*, vol. 78, no. 2, pp. 233–240, 2009.
- [29] C. S. Holling, “The components of predation as revealed by a study of small-mammal predation of the european pine sawfly,” *The Canadian Entomologist*, vol. 91, no. 5, pp. 293–320, 1959.
- [30] J. M. Jeschke, M. Kopp, and R. Tollrian, “Predator functional responses: discriminating between handling and digesting prey,” *Ecological Monographs*, vol. 72, no. 1, pp. 95–112, 2002.
- [31] M. J. Smith and D. G. Harper, “Animal signals: models and terminology,” *Journal of theoretical biology*, vol. 177, no. 3, pp. 305–311, 1995.
- [32] C. D. FitzGibbon and J. H. Fanshawe, “Stotting in thomson’s gazelles: an honest signal of condition,” *Behavioral Ecology and Sociobiology*, vol. 23, no. 2, pp. 69–74, 1988.
- [33] V. Csányi and A. Dóka, “Learning interactions between prey and predator fish,” *Marine & Freshwater Behaviour & Phy*, vol. 23, no. 1-4, pp. 63–78, 1993.

- [34] C. Brown and K. N. Laland, “Social learning in fishes: a review,” *Fish and fisheries*, vol. 4, no. 3, pp. 280–288, 2003.
- [35] R. Boyd and P. J. Richerson, *Culture and the evolutionary process*. University of Chicago press, Chicago USA, 1988.
- [36] M. Weinstock, “The long-term behavioural consequences of prenatal stress,” *Neuroscience and Biobehavioral Reviews*, vol. 32, pp. 1073–1086, 2008.
- [37] S. J. Schoech, M. A. Rensel, and R. S. Heiss, “Short and long-term effects of developmental corticosterone exposure on avian physiology, behavioral phenotype, cognition, and fitness: review,” *Current Zoology*, vol. 57, no. 4, pp. 514–530, 2011.
- [38] S. Maccari, H. J. Krugers, S. Morley-Fletcher, M. Szyf, and P. J. Brunton, “The consequences of early-life adversity: neurobiological, behavioural and epigenetic adaptations,” *Journal of Neuroendocrinology*, vol. 26, pp. 707–723, 2014.
- [39] M. G. Crandall and P. H. Rabinowitz, “Mathematical theory of bifurcation,” in *Bifurcation Phenomena in Mathematical Physics and Related Topics* (C. Bardos and D. Bessis, eds.), (Dordrecht), pp. 3–46, Springer Netherlands, 1980.
- [40] P. H. Rabinowitz, “Some global results for nonlinear eigenvalue problems,” *Journal of Functional Analysis*, vol. 7, no. 3, pp. 487–513, 1971.
- [41] M. Golubitsky and D. G. Schaeffer, *Singularities and Groups in Bifurcation Theory*, vol. I. New York: Springer, 1985.
- [42] T. Ma and S. Wang, *Bifurcation Theory and Applications*, vol. 53 of *World Scientific Series on Nonlinear Science A*. Singapore: World Scientific Publishing, 2005.
- [43] M. Krasnoselskii and P. Zabreiko, *Geometrical Methods of Nonlinear Analysis*. New York: Springer, 1984.
- [44] J. M. Cushing, *An Introduction to Structured Population Dynamics*. CBMS-NSF Conference Series in Applied Mathematics, Philadelphia: Society for Industrial and Applied Mathematics, 1988.
- [45] K. P. Wijaya, Sutimin, E. Soewono, and T. Götz, “On the existence of a nontrivial equilibrium in relation to the basic reproductive number,” *Journal of Applied Mathematics and Computer Science*, vol. 27, no. 3, pp. 623–636, 2017.
- [46] H. Dankowicz and F. Schilder, *Recipes for continuation*. Computational Science and Engineering, Philadelphia: SIAM, 2013.
- [47] E. J. Doedel, A. R. Champneys, T. F. Fairgrieve, Y. A. Kuznetsov, B. Sandstede, and X.-J. Wang, *Auto97: Continuation and bifurcation software for ordinary differential equations (with HomCont)*. Computer Science, Concordia University, Montreal, Canada, 1997. Available at <http://cmvl.cs.concordia.ca>.
- [48] A. Dhooge, W. Govaerts, and Y. A. Kuznetsov, “MATCONT: A MATLAB package for numerical bifurcation analysis of ODEs,” *ACM Trans. Math. Software*, vol. 29, no. 2, pp. 141–164, 2003.
- [49] J. Guckenheimer and P. Holmes, *Nonlinear Oscillations, Dynamical Systems, and Bifurcations of Vector Fields*, vol. 42 of *Applied Mathematical Sciences*. New York: Springer-Verlag, 1993. Fourth printing.
- [50] W. Govaerts, *Numerical Methods for Bifurcations of Dynamical Equilibria*. Philadelphia: SIAM, 2000.

- [51] C. M. Kribs-Zaleta and J. X. Velasco-Hernández, “A simple vaccination model with multiple endemic states,” *Mathematical Biosciences*, vol. 164, no. 2, pp. 183–201, 2000.
- [52] P. van den Driessche and J. Watmough, “A simple SIS epidemic model with a backward bifurcation,” *J. Math. Biol.*, vol. 40, no. 6, pp. 525–540, 2000.
- [53] M. Liu, E. Liz, and G. Röst, “Endemic bubbles generated by delayed behavioral response: Global stability and bifurcation switches in an SIS model,” *SIAM J. Appl. Math.*, vol. 75, no. 1, pp. 75–91, 2015.